Published in final edited form as:
Vision Res. 2010 March 17; 50(6): 614–622. doi:10.1016/j.visres.2010.01.009.

Responses and Receptive Fields of Amacrine Cells and Ganglion Cells in the Salamander Retina

Ai-Jun Zhang and **Samuel M. Wu**
Cullen Eye Institute, Baylor College of Medicine, Houston, Texas 77030

Abstract

Retinal amacrine cells (ACs) and ganglion cells (GCs) have been shown to display large morphological diversity, and here we show that four types of ACs and three types of GCs exhibit physiologically-distinguishable properties. They are the sustained ON ACs; sustained OFF ACs; transient ON-OFF ACs; transient ON-OFF ACs with wide receptive fields; sustained ON-center/OFF-surround GCs; sustained OFF-center/ON-surround GCs and transient ON-OFF GCs. By comparing response waveforms, receptive fields and relative rod/cone inputs of ACs and GCs with the corresponding parameters of various types of the presynaptic bipolar cells (BCs), we analyze how different types of BCs mediate synaptic inputs to various ACs and GCs. Although more types of third-order retinal neurons may be identified by more refined classification criteria, our observations suggest that many morphologically-distinct ACs and GCs share very similar physiological responses.

Keywords

center-surround antagonistic receptive fields; dendritic fields; relative rod/cone inputs; response waveforms; spatial information processing; electrical coupling

Introduction

In the vertebrate retina, the primary information channels are the photoreceptors-bipolar cells (BCs)-ganglion cells (GCs) synaptic pathways, which convey rod and cone signals to the brain (Dowling, 1987). The lateral channels include the cone-horizontal cell (HC) feedback synapse, the HC-BC feedforward synapse, the amacrine cell (AC)-BC feedback synapse and the AC-GC feedforward synapse (Wu, 1994;Zhang and Wu, 2009a). Cones, BCs and GCs exhibit center-surround antagonistic receptive field (CSARF) organization (Werblin and Dowling, 1969;Kaneko, 1970;Kuffler, 1953), the basic template for spatial information processing in the visual system (Hubel and Wiesel, 1962). Center responses are mediated by the photoreceptor-BC-GC channels, whereas the surround responses are mediated by the lateral HC and AC feedback and feedforward synapses (Werblin and Dowling, 1969).

Correspondance: Samuel M. Wu, Ph.D., Cullen Eye Institute, Baylor College of Medicine, One Baylor Plaza, NC-205, Houston, TX 77030. Tel: (713) 798-5966, Fax: (713) 798-6457, swu@bcm.tmc.edu.

In earlier studies, we characterized the response waveforms, relative rod/cone input, receptive field properties and patterns of dye coupling of the A- and B-type HCs (Zhang et al., 2006a;Zhang et al., 2006b) and six types of BCs (Zhang and Wu, 2009a) in the salamander outer retina. Here we continue our studies by correlating response, receptive field and morphological properties of various types of ACs and GCs. We also compare results obtained with cell morphology and light response characteristics of ACs and GCs under voltage clamp recorded in living retinal slices, in which the cells' receptive fields could not be measured (Pang et al., 2002b;Pang et al., 2002a). Since ACs and GCs are postsynaptic to BCs, by comparing response waveforms, receptive fields and relative rod/cone inputs of ACs and GCs with the corresponding parameters of BCs, we are able to postulate how various types of BCs mediate synaptic inputs to different types of ACs and GCs.

It has been shown that vertebrate retinal ACs and GCs exhibit large morphological diversity (MacNeil and Masland, 1998;Sun et al., 2002;Cleland et al., 1975). However, it is not clear whether each of the morphologically-distinguishable ACs and GCs represents a physiologically distinct type of neuron. In this study, we examined the response waveforms, receptive field properties, relative rod/cone inputs and morphology of 43 ACs and 40 GCs in dark-adapted flat-mounted salamander retinas, and found that the numbers of physiologically-distinguishable AC and GC types are significantly less than the numbers of morphological types, suggesting that many of the morphological types of ACs and GCs may share similar physiological responses.

Methods

Flat-mounted, isolated retinas of larval tiger salamanders (*Ambystoma tigrinum*) purchased from Charles E. Sullivan, Co. (Nashville, TN) and KON's Scientific Co. Inc. (Germantown, WI) were used in this study. Animals were handled in accordance with the policies on treatment of laboratory animals of Baylor College of Medicine and the National Institutes of Health. Detailed experimental procedures were described in previous publications (Yang and Wu, 1989;Zhang et al., 2006a). Prior to an experiment, the animal was dark-adapted for at least one hour and then decapitated and dissected under infrared illumination with a dual-unit Nitemare (BE Meyers, Redmond, WA). Oxygenated Ringer's solution was introduced to the superfusion chamber at a rate of about five ml/minute, so that the retina was immersed totally under solution. The control Ringer's contained 108 mM NaCl, 2.5 mM KCl, 1.2 mM $MgCl_2$, 2 mM $CaCl_2$, 5 mM Hepes (adjusted at pH 7.7).

Intracellular recordings were made with micropipettes drawn out on a modified Livingstone puller or Sutter microelectrode puller with single barrel omega dot tubing. The pipettes were filled with 2M potassium acetate and have resistance, measured in Ringer's solution of 100-600 MΩ. Amacrine cells and ganglion cells were recorded with a microelectrode amplifier (MEZ-8300, Nihon Kohden). For cell morphology and dye coupling studies, microelectrode tips were filled with 3% Neurobiotin in 50 mM Tris and backfilled with 3 M lithium chloride. After physiological experiments, dyes were injected with positive and negative currents (1-5 nA, 3 Hz, 30 min). Then the tissues were fixed with 4% paraformaldehyde for two hours and were subsequently immunolabeled with strepavidin conjugated Cy-3. Cell morphology and patterns of dye coupling were visualized with a confocal microscope (Zeiss 510).

A new computer-controlled, dual-beam light stimulator with an automated projector head was constructed for experiments that require center and surround light stimuli in flat-mounted retinas. Both light beams pass through interference filters, neutral density filters and apertures of various configurations mounted on motorized wheels controlled by the

computer. The receptive field of a given cell was mapped by a moving light bar through the automated projector head in two orthogonal directions, and the cell's receptive field center was determined by the intersecting point of the maximum responses to the light bar in the two directions. The receptive field diameter was estimated by the distance between the light bar positions that generate 5% of the cell's maximum responses. The center light spot (with various diameters) and a concentric surround light annulus (with various inner and outer diameters) were projected to the retina. The intensity of unattenuated 500 nm light (log I = 0) is 2.05×10^7 photons μm^{-2} sec^{-1}.

Results

Response waveforms, morphology, receptive field properties of four types of amacrine cells

Forty-three ACs in the dark-adapted flat-mounted tiger salamander retina were recorded with microelectrodes. ACs are identified by their soma depth (in the proximal half of the inner nuclear layer), dendritic morphology and that they do not bear axons, when viewed after Neurobiotin filling. Four major AC types were distinguished, according to their response waveform, morphology and receptive field properties. The first type is the sustained ON ACs (sON-ACs, N=10), as shown in Figure 1, which illustrates the voltage responses to a whole-field light step and center/surround illuminations (A), morphology (B), responses to a stepwise moving light bar (C) and to a continuous moving bar in two opposite directions (D). The response-intensity (V-Log I) curves of the responses to 500 nm and 700nm lights are shown in (E), which give a spectral difference (ΔS, defined as $S_{700} - S_{500}$ (where S_{700} and S_{500} are intensities of 700 nm and 500 nm light eliciting responses of the same amplitude) (Yang and Wu, 1990)) of 0.91 (average = 1.15±0.69), indicative of a cone-dominated or rod/cone mixed light input. Neurobiotin staining reveals a dendritic field diameter (DFD) of 420 μm (average = 428±197 μm), and no indications of dye coupling with adjacent cells. These cells exhibited an average receptive field diameter (RFD) of 435±219 μm, and no center-surround antagonism (CSA) or directional selectivity was observed.

The second type is the sustained OFF ACs (sOFF-ACs, N=11), as shown in Figure 2. These cells exhibited a sustained hyperpolarizing response to a whole-field light step, a transient OFF overshoot response, followed by a hyperpolarizing voltage tail, and they did not show center-surround antagonism (Figure 2A). Neurobiotin staining reveals a DFD of 392 μm (average = 408±188 μm), and no indications of dye coupling with adjacent cells (Figure 2B). Responses to moving light bars indicate an average RFD of 406±247 μm (C) without directional selectivity (D). The response-intensity (V-Log I) curves give a spectral difference of 1.11 (with an average of 1.49±0.45), indicative of a mixed rod/cone light input (Pang et al., 2004).

The third type is the transient ON-OFF ACs (tON/OFF-ACs, N=10), as shown in Figure 3. These cells exhibited transient depolarizing responses at the onset and offset of the whole-field light step, and they did not show center-surround antagonism (Figure 3A). Neurobiotin staining reveals a DFD of 687 μm (average = 668±226 μm), and no indications of dye coupling with adjacent cells (Figure 3B). Responses to moving light bars give a RFD of 707±286 μm (C) without directional selectivity (D). The response-intensity (V-Log I, E) curves yield a spectral difference of 1.35 for the ON response (average ΔS for ON and OFF are 1.51±0.32 and 1.30±0.27, respectively), indicating both ON and OFF are mediated by mixed rod/cone light inputs.

The fourth type is the transient ON-OFF ACs with wide dendritic fields (tON/OFF-ACw, N=12), as shown in Figure 4. These cells exhibited transient spike-like depolarizing

responses at the onset and offset of the whole-field light step, followed by a burst of transient depolarizing events (after potential (Yang et al., 2002), Figure 4A and insert), and they did not show center-surround antagonism (Figure 4A). Neurobiotin staining reveals a DFD of 1,654 μm (average = 1,708±278 μm), and they are dye coupled with many adjacent cells (Figure 4B). Responses to moving light bars give an average RFD of 1,800±186 μm (C) without directional selectivity (D). The response-intensity (V-Log I) curves yield a spectral difference of 1.83 for the ON response (average ΔS for ON and OFF are 1.73±0.51 and 1.54±0.40, respectively), indicating both ON and OFF are mediated by mixed rod/cone light inputs.

Amacrine cell types, their response waveforms, average spectral differences, average dendritic and receptive field diameters, as well as presence or absence of center surround antagonism and dye coupling are summarized in Table 1.

Response waveforms, morphology, receptive field properties of three types of ganglion cells

Forty GCs in the dark-adapted flat-mounted tiger salamander retina were recorded with microelectrodes, and they are identified by their soma depth (in GC layer), dendritic morphology and the presence of axons when filled with Neurobiotin. Three major GC types were found, based on their response waveform, relative rod/cone inputs, morphology and receptive field properties. The first type is the sustained ON-center/OFF-surround GCs (sON-c-GCs, N=15), as shown in Figure 5, which illustrates the voltage responses to a whole-field light step and center/surround illuminations (A), morphology revealed by Neurobiotin filling (B), responses to a stepwise moving light bar (C) and to a continuous moving bar in two opposite directions (D). The response-intensity (V-Log I) curves (E) give a spectral difference for the center response of 1.8 (average = 1.77±0.68), indicative of a mixed rod/cone light input. Neurobiotin staining reveals a DFD of 563 μm (average = 577±190 μm), and no indications of dye coupling with adjacent cells. The cell exhibited an average receptive field center diameter (RFCD) of 585±166 μm, and no directional selectivity. They show clear ON-center/OFF-surround antagonism, with a depolarizing response and increase of spike activity to center light spot and a hyperpolarizing response and decrease of spike to surround light annulus (A).

The second type is the sustained OFF-center/ON-surround GCs (sOFF-c-GCs, N=14), as shown in Figure 6. These cells exhibited spontaneous spike activity in darkness, a sustained hyperpolarizing response and decrease of spike activity to a whole-field light step, a hyperpolarizing response and decrease of spike activity to center light spot and a depolarizing response and increase of spike to surround light annulus (Figure 6A). Neurobiotin staining reveals a DFD of 800 μm (average = 778±144 μm), and no indications of dye coupling with adjacent cells (Figure 6B). Responses to moving light bars give a RFCD of 830±123 μm without directional selectivity (Figure 6C-D). The response-intensity (V-Log I) curves give a spectral difference for the center response of 1.20 (with an average of 1.29±0.68), indicative of a mixed rod/cone light input.

The third type is the transient ON-OFF GCs (tON/OFF-GCs, N=11), as shown in Figure 7. These cells exhibited transient depolarizing responses and increase of spike activity at the onset and offset of the whole-field light step, followed by a burst of spikes (after potential (Yang et al., 2002) Figure 7A and insert), and they did not show center-surround antagonism (Figure 7A). Neurobiotin staining reveals a DFD of 708 μm (average = 697±254 μm), and they are dye coupled with many adjacent cells (Figure 7B). Responses to moving light bars indicate an average receptive field diameter of 2,170±311 μm without directional selectivity (Figure 7C-D). The response-intensity (V-Log I) curves (Figure 7E) give a spectral difference of 2.5 (with an average of 2.20±1.03) for the ON responses and 0.81 (average =

0.91±0.71) for the OFF responses, indicating that the ON responses are rod-dominated and the OFF responses are cone-dominated.

Ganglion cell types, their response waveforms, average spectral differences, average dendritic and receptive field diameters, as well as presence/absence of center surround antagonism and dye coupling are summarized in Table 1.

Relative rod/cone inputs and receptive field properties of BCs, ACs and GCs in dark-adapted salamander retina

Figure 8 shows scatter plots of receptive field diameter versus spectral difference ΔS of the 4 types of ACs and 3 types of GCs described above, as well as the DBCs and HBCs in a previous publication (Zhang and Wu, 2009a). It is evident that all four types of ACs and the ON-center/OFF-surround and OFF-center/ON-surround GCs receive mixed rod/cone inputs, as their ΔS values are between 1.0 and 2.0 (Pang et al., 2004;Zhang and Wu, 2009a). The light responses of these cells are therefore likely be mediated by DBCs and HBCs with mixed rod/cone inputs (DBC_Ms and HBC_Ms) and/or combinations of rod-dominated and cone-dominated DBCs/HBCs. Although the ON and OFF responses of both types of ON-OFF ACs fall in the mixed rod/cone range, the ON responses are more rod-dominated than the OFF responses. The ON and OFF responses of the ON-OFF GCs exhibit very distinct rod/cone dominance: the ON responses are largely mediated by rod-dominated BCs (DBC_Rs) and the OFF responses are mainly mediated by cone-dominated BCs (HBC_Cs).

Figure 8 also reveals that the DFDs of the first 3 types of ACs and the first two types of GCs are below 1,000 μm, and the DFDs of the fourth type of ACs and the third type of GCs are larger than 1,500 μm. Implications of the relative rod/cone inputs and receptive field sizes of ACs, GCs and BCs will be discussed below.

Discussion

AC response waveform, relative rod/cone input, dendritic fields and receptive fields

We have presented in this article four types of ACs with distinct light response and receptive field properties in dark-adapted salamander retina. The first three have DFDs and RFDs between 400 and 1,000 μm with sustained ON, sustained OFF and transient ON-OFF light responses, whereas the fourth has RFDs and RFDs >1,500 μm with transient ON-OFF light response. In the first 3 types of ACs, the DFDs measured by dye filling and the RFDs measured physiologically are of comparable sizes, and no dye coupling was observed, suggesting light-evoke voltage responses of these cells are mediated largely by their own dendritic inputs. In the fourth type, dye coupling is observed in adjacent cells, but the identities of these cells are not determined. Additionally, all four types of ACs exhibit mixed rod/cone inputs, indicating that their light responses are mediated by BCs of mixed rod/cone inputs (HBC_Ms and DBC_Ms) and/or by combinations of rod-dominated BCs (HBC_Rs and DBC_Rs) and cone-dominated BCs (HBC_Cs and DBC_Cs) (Zhang and Wu, 2009a).

BC density in the tiger salamander retina is estimated to be about 4,000/mm^2 (Zhang and Wu, 2009b), and therefore an AC dendritic/receptive field area (DFD: 400-1,700 μm gives dendritic field area ($\pi(DFD/2)^2$): 0.126-2.27 mm^2) covering about 500-9,000 BCs. The average dendritic field diameter (DFD) of BCs is about 60 μm (Wu et al., 2000), and because of homocellular coupling, the receptive field centers of various types of BCs range from 300 to 500 μm (see Figure 8) (Zhang and Wu, 2009a). Since the RFDs of the first 3 types of ACs are only slightly larger than the average BC RFCD, these ACs should only receive synaptic inputs from BCs of the same response polarity near the ACs' receptive field center (sustained ON AC from DBCs, sustained OFF from HBCs and transient ON-OFF ACs from both DBCs and HBCs). The reason for this is that if BCs beyond the center region

of the AC did send synaptic inputs, the AC's RFD would have been substantially larger than the BC's RFD. The wide-field ON-OFF ACs, on the other hand, could receive synaptic inputs from many DBCs and HBCs. An AC of RFD of 1,700 μm, for example, may receive synaptic inputs from BCs whose somas are located 650 μm away from the AC RF center.

Our results show that none of the 4 AC types exhibit center-surround antagonistic receptive fields (CSARFs), whereas all BCs, their input neurons, display CSARFs (Zhang and Wu, 2009a). This is understandable for the wide-field ON-OFF ACs (tON/OFF-ACws) because they receive synaptic inputs from many BCs spreading widely in the ACs' dendritic field and thus the center and surround antagonistic responses may cancel each other. It is also reasonable for the tON/OFF-ACs not to display CSARFs because even though they receive inputs from BCs near the AC RF center, these BCs are both DBCs and HBCs, and thus the surround responses from the two BC types may cancel each other. Our observation that the sON-ACs and sOFF-ACs does not exhibit CSARFs is somewhat puzzling, as they receive inputs from BCs of the same polarity near their RF center. It is possible some special synaptic arrangements, such as AC-AC interactions (Zhang et al., 1997), are used to suppress the antagonistic surround responses in these ACs.

In this report, we identify four types of ACs in the flat-mounted salamander retina, based on their distinct physiological properties such as light response waveform, receptive field size and relative rod/cone inputs. In an earlier whole-cell voltage clamp study in retinal slices, we correlated the morphology (especially patterns and levels of dendritic ramification in the IPL) with light response characteristics of many types of salamander ACs (Pang et al., 2002b). It is evident that the present study "lumps" many morphologically-distinct types of ACs into single physiological types according to their receptive field sizes, response waveforms and relative rod/cone inputs. One exception is that a number of ACs in retinal slices are "narrow field" cells (DFD < 200 μm (Pang et al., 2002b)) whereas our present work in the flatmount retina does not show such ACs. One hypothesis for this discrepancy is that the apparent "narrow" dendritic trees in retinal slices result from slicing-induced dendritic cleavage. Another possibility is that microelectrodes used in this study is "biased" against impaling these narrow-field ACs.

GC response waveform, relative rod/cone input, dendritic fields and receptive fields

We have identified three types of GCs with distinct light response and receptive field properties in dark-adapted salamander retina. They are the medium-field (RFD between 580 and 800 μm) cells with sustained ON-center, sustained OFF-center and wide-field (RFD >1,500 μm) transient ON-OFF light responses. The dendritic field diameters of the first two types of GCs are of comparable size with their receptive field diameters, and no dye coupling was observed when they were filled with Neurobiotin, suggesting light-evoke voltage responses of these cells are mediated largely by their own dendritic inputs. The receptive field diameters of the third type of GCs are much larger than their dendritic field diameter, and strong dye coupling was observed in nearby cells when the recorded cells were filled with Neurobiotin. This result suggests that the light responses of the tON/OFF-GCws are not only mediated by their own dendritic inputs, but also by adjacent cells via electrical coupling.

The sustained ON-center GCs and sustained OFF-center GCs exhibit mixed rod/cone inputs, suggesting that their light responses are mediated by BCs of mixed rod/cone inputs (HBC_Ms and DBC_Ms) and/or by combinations of rod-dominated BCs (HBC_Rs and DBC_Rs) and cone-dominated BCs (HBC_Cs and DBC_Cs) (Zhang and Wu, 2009a). The ON responses of the transient ON-OFF GCs are generated by rod-dominated inputs whereas the OFF responses are generated by cone-dominated inputs (Hensley et al., 1993). Therefore these GCs are likely to receive synaptic inputs mainly from DBC_Rs and HBC_Cs.

By using similar analysis as in the previous section for ACs, we found that the RFDs of the sustained ON-center and sustained OFF-center GCs are about 1.5-2.5 time larger than the average BC RFCD, thus these GCs should only receive synaptic inputs from BCs of the same response polarity near the GCs' receptive field center (sustained ON-center GC from DBCs, sustained OFF-center GCs from HBCs). The wide-field ON-OFF GCs, on the other hand, may receive synaptic inputs from many DBCs and HBCs within the dendritic fields of their own and in the coupled network.

In contrast to the sustained ACs, the sustained ON-center and sustained OFF-center GCs exhibit center-surround antagonism (CSA). This is consistent with the idea that these GCs receive inputs from BCs of the same polarity near their receptive field center, and thus not only the center, but also the antagonistic surround receptive fields are preserved. This of course does not imply, however, that the GC surround responses are completely inherited from BC surround responses. AC→GC feedforward lateral synapses are additional contributors of the GC surround responses (Werblin, 1972;Cook and McReynolds, 1998). The wide-field ON-OFF GCs, like the wide-field ON-OFF ACs, do not show CSA because they receive synaptic inputs from many BCs spreading widely in the GCs' dendritic field and thus the center and surround antagonistic responses cancel one another.

The three types of GCs obtained from the flat-mounted salamander retina reported here are consistent with the results obtained from a whole-cell voltage clamp study in retinal slices (Pang et al., 2002a) and an extracellular recording study in whole retinas (Hensley et al., 1993). All three studies demonstrate 3 major types of GCs with distinct morphology (dendrites of ON-center GCs ramify in the proximal half of the IPL, dendrites of OFF-center GCs ramify in the distal half of the IPL, and dendrites of ON-OFF GCs ramify in both halves of the IPL), light response waveforms and relative rod/cone inputs (Pang et al., 2002a). It is quite possible that these three types of GCs "lump" many GCs with different morphology. However, the present study with the additional receptive field information helps to confirm that there are the three major physiological types of retinal GCs in the salamander retina.

It is important to note that although the ACs and GCs described in this paper represent major third-order neurons in the salamander retina, more types of ACs and GCs may be identified, when more refined classification criteria are applied. For example, although the voltage responses of the medium-field transient ON-OFF ACs are very similar, they may be mediated by postsynaptic light-evoked cation and chloride current responses (ΔI_C and ΔI_{Cl}) of different strengths (Pang et al., 2002b). Additionally, the sustained ON-center GCs may exhibit similar center-surround responses, but they may differ from one another by using either the AC-BC-GC feedback synapse, the AC-GC feedforward synapse or different combinations of the two to mediate the surround responses (Zhang and Wu, 2009a). It is also possible that more physiologically-distinct ACs and GCs will surface when the cell pool size is much larger. A large-scale, voltage-clamp (for separating ΔI_C and ΔI_{Cl}) investigation with pharmacological tools (for separating feedback and feedforward lateral inputs) is needed for further classification of ACs and GCs in this retina.

Acknowledgments

We thank Andrew Barrow and Roy Jacoby for critically reading this manuscript. This work was supported by grants from NIH (EY 04446), NIH Vision Core (EY 02520), the Retina Research Foundation (Houston), and the Research to Prevent Blindness, Inc.

Reference List

Cleland BG, Levick WR, Wassle H. Physiological identification of a morphological class of cat retinal ganglion cells. J Physiol. 1975; 248:151–171. [PubMed: 1151804]

Cook PB, McReynolds JS. Lateral inhibition in the inner retina is important for spatial tuning of ganglion cells. Nat Neurosci. 1998; 1:714–719. [PubMed: 10196588]

Dowling, JE. The Retina, an Approachable Part of the Brain. Harvard University Press; 1987.

Hensley SH, Yang XL, Wu SM. Relative contribution of rod and cone inputs to bipolar cells and ganglion cells in the tiger salamander retina. J Neurophysiol. 1993; 69:2086–2098. [PubMed: 8350133]

Hubel DH, Wiesel TN. Receptive field, binocular interactionand functional architecture in the cat's visual cortex. J Physiol. 1962; 160:106–154. [PubMed: 14449617]

Kaneko A. Physiological and morphological identification of horizontal, bipolar and amacrine cells in goldfish retina. J Physiol. 1970; 207:623–633. [PubMed: 5499739]

Kuffler SW. Discharge patterns and functional organization of the mammalian retina. J Neurophysiol. 1953; 16:37–68. [PubMed: 13035466]

MacNeil MA, Masland RH. Extreme diversity among amacrine cells: implications for function. Neuron. 1998; 20:971–982. [PubMed: 9620701]

Pang JJ, Gao F, Wu SM. Relative contributions of bipolar cell and amacrine cell inputs to light responses of ON, OFF and ON-OFF retinal ganglion cells. Vision Res. 2002a; 42:19–27. [PubMed: 11804628]

Pang JJ, Gao F, Wu SM. Segregation and integration of visual channels: layer-by-layer computation of ON-OFF signals by amacrine cell dendrites. J Neurosci. 2002b; 22:4693–4701. [PubMed: 12040076]

Pang JJ, Gao F, Wu SM. Stratum-by-stratum projection of light response attributes by retinal bipolar cells of Ambystoma. J Physiol. 2004; 558:249–262. [PubMed: 15146053]

Sun W, Li N, He S. Large-scale morphological survey of mouse retinal ganglion cells. J Comp Neurol. 2002; 451:115–126. [PubMed: 12209831]

Werblin FS. Lateral interactions at inner plexiform layer of vertebrate retina: antagonistic responses to change. Science. 1972; 175:1008–1010. [PubMed: 5009392]

Werblin FS, Dowling JE. Organization of the retina of the mudpuppy, Necturus maculosus. II. Intracellular recording. J Neurophysiol. 1969; 32:339–355. [PubMed: 4306897]

Wu SM. Synaptic transmission in the outer retina. Annu Rev Physiol. 1994; 56:141–168. [PubMed: 8010738]

Wu SM, Gao F, Maple BR. Functional architecture of synapses in the inner retina: segregation of visual signals by stratification of bipolar cell axon terminals. J Neurosci. 2000; 20:4462–4470. [PubMed: 10844015]

Yang XL, Gao F, Wu SM. Non-linear, high-gain and sustained-to-transient signal transmission from rods to amacrine cells in dark-adapted retina of Ambystoma. J Physiol. 2002; 539:239–251. [PubMed: 11850516]

Yang XL, Wu SM. Effects of background illumination on the horizontal cell responses in the tiger salamander retina. J Neurosci. 1989; 9:815–827. [PubMed: 2538583]

Yang XL, Wu SM. Synaptic inputs from rods and cones to horizontal cells in the tiger salamander retina. Sci China B. 1990; 33:946–954. [PubMed: 2242218]

Zhang AJ, Wu SM. Receptive fields of retinal bipolar cells are mediated by heterogeneous synaptic circuitry. J Neurosci. 2009a; 29:789–797. [PubMed: 19158304]

Zhang AJ, Zhang J, Wu SM. Electrical coupling, receptive fields, and relative rod/cone inputs of horizontal cells in the tiger salamander retina. J Comp Neurol. 2006a; 499:422–431. [PubMed: 16998920]

Zhang J, Jung CS, Slaughter MM. Serial inhibitory synapses in retina. Vis Neurosci. 1997; 14:553–563. [PubMed: 9194322]

Zhang J, Wu SM. Immunocytochemical analysis of photoreceptors in the tiger salamander retina. Vision Res. 2009b; 49:64–73. [PubMed: 18977238]

Zhang J, Zhang AJ, Wu SM. Immunocytochemical analysis of GABA-positive and calretinin-positive horizontal cells in the tiger salamander retina. J Comp Neurol. 2006b; 499:432–441. [PubMed: 16998928]

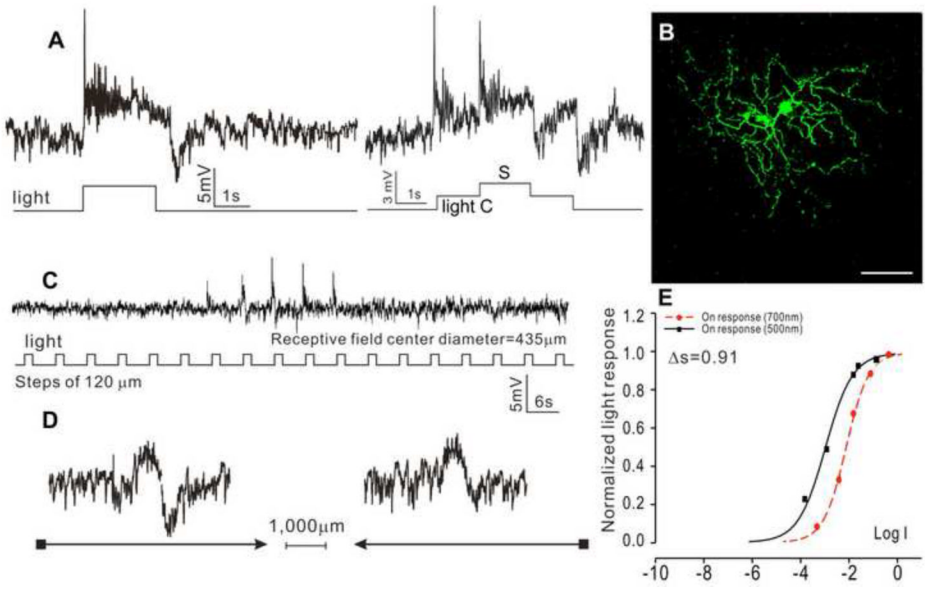

Figure 1.

(A) Voltage responses of a sustained ON AC (sON-AC) elicited by whole-field light step (-3, 500 nm) and by a center light spot (300 μm) and a surround light annulus (700 μm inner diameter, 2,000 μm outer diameter) recorded from dark-adapted salamander flatmounted retinas. ΔS of this AC is 0.91. (B) Fluorescent micrographs of the AC soma and dendrites (confocal images of the inner INL and IPL) stained with neurobiotin (green) by 10-minute dye injection. Dendritic field diameter (DFD) is 420 μm. Calibration bar: 100μm. (C) Voltage responses of the AC to a light bar moving stepwise (with 120 μm step increments) across the receptive field. The receptive field diameter (RFD) is 435μm. (D) Voltage responses to a moving light bar in the x and –x directions.

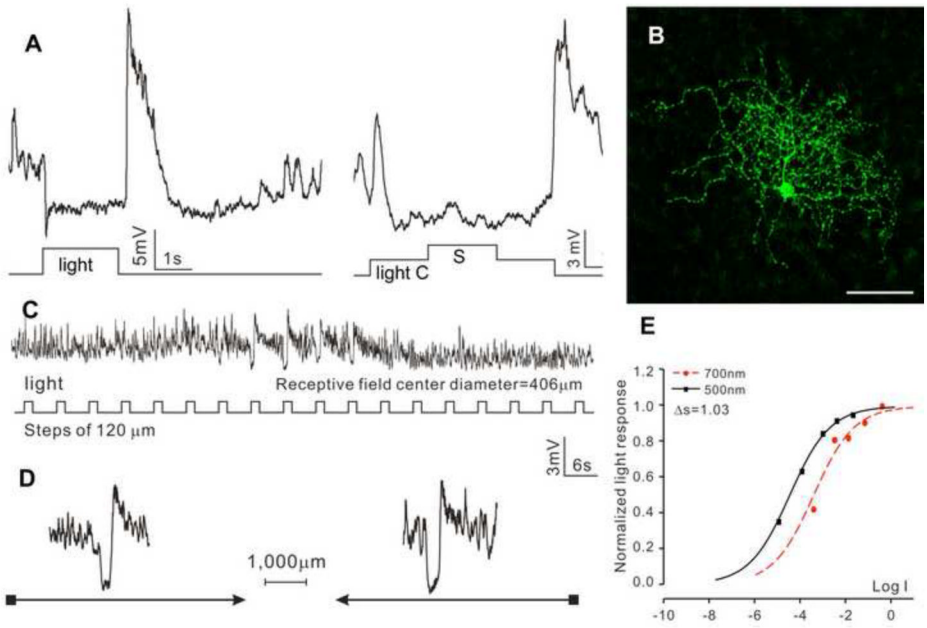

Figure 2.

(A) Voltage responses of a sustained OFF AC (sOFF-AC) elicited by whole-field light step (-3, 500 nm) and by a center light spot (300 μm) and a surround light annulus (700 μm inner diameter, 2,000 μm outer diameter) recorded from dark-adapted salamander flatmounted retinas. ΔS of this AC is 1.03. (B) Fluorescent micrographs of the AC soma and dendrites (confocal images of the inner INL and IPL) stained with neurobiotin (green) by 10-minute dye injection. Dendritic field diameter is 392 μm. Calibration bar: 100μm. (C) Voltage responses of the AC to a light bar moving stepwise (with 120 μm step increments) across the receptive field. The receptive field diameter (RFD) is 406μm. (D) Voltage responses to a moving light bar in the x and –x directions.

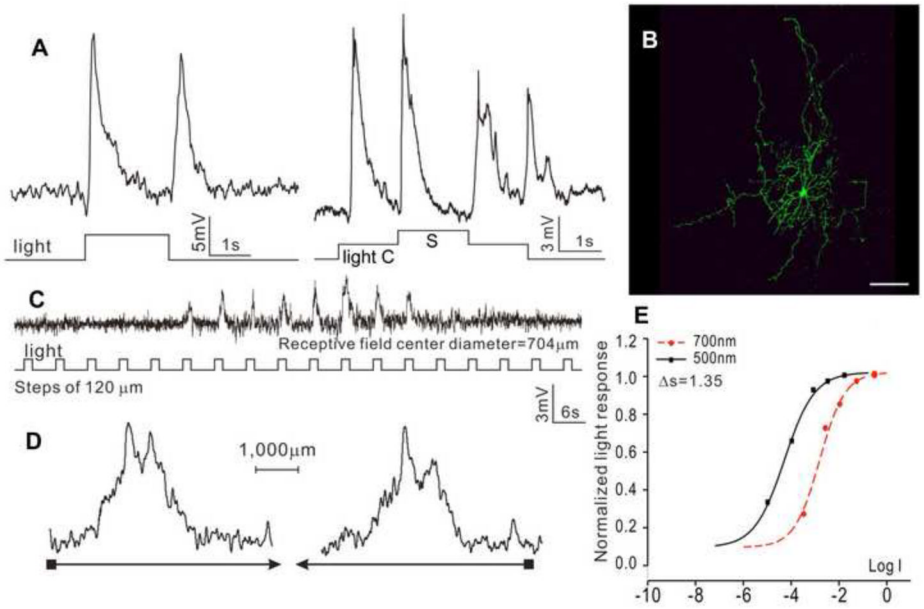

Figure 3.

(A) Voltage responses of a medium-field, transient ON-OFF AC (tON/OFF-AC) elicited by whole-field light step (-3, 500 nm) and by a center light spot (300 μm) and a surround light annulus (700 μm inner diameter, 2,000 μm outer diameter) recorded from dark-adapted salamander flatmounted retinas. ΔS of this AC is 1.35. (B) Fluorescent micrographs of the AC soma and dendrites (confocal images of the inner INL and IPL) stained with neurobiotin (green) by 10-minute dye injection. Dendritic field diameter is 687 μm. Calibration bar: 100μm. (C) Voltage responses of the AC to a light bar moving stepwise (with 120 μm step increments) across the receptive field. The receptive field diameter (RFD) is 704μm. (D) Voltage responses to a moving light bar in the x and –x directions.

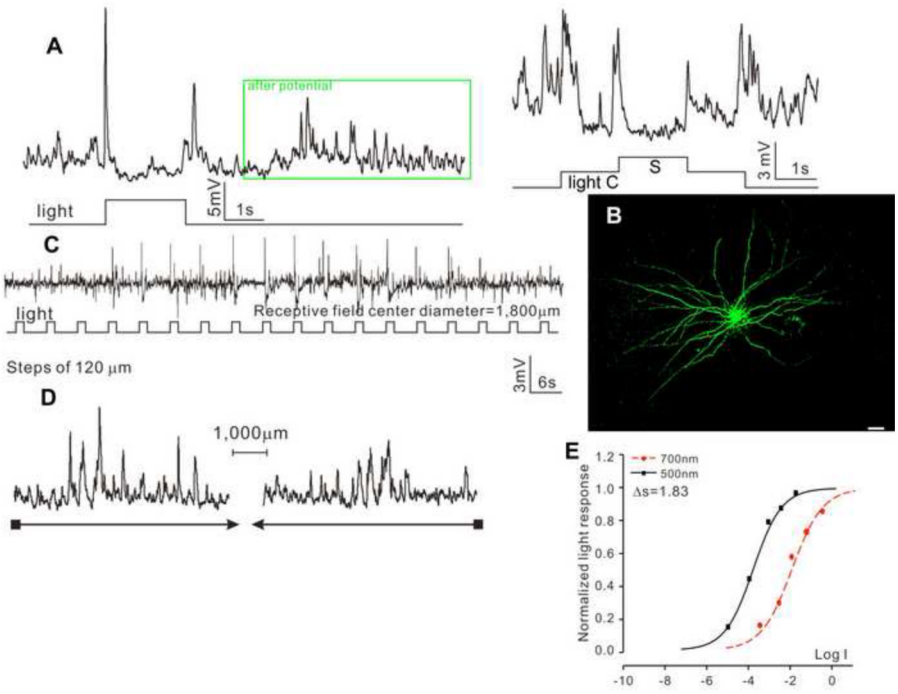

Figure 4.

(A) Voltage responses of a transient ON-OFF AC with wide receptive field (tON/OFF-ACw) elicited by whole-field light step (-3, 500 nm) and by a center light spot (300 μm) and a surround light annulus (700 μm inner diameter, 2,000 μm outer diameter) recorded from dark-adapted salamander flatmounted retinas. ΔS of this AC is 1.83. (B) Fluorescent micrographs of the AC soma and dendrites (confocal images of the inner INL and IPL) stained with neurobiotin (green) by 10-minute dye injection. Dendritic field diameter is 1,654 μm. Calibration bar: 100μm. (C) Voltage responses of the AC to a light bar moving stepwise (with 120 μm step increments) across the receptive field. The receptive field diameter (RFD) is 1,800μm. (D) Voltage responses to a moving light bar in the x and –x directions.

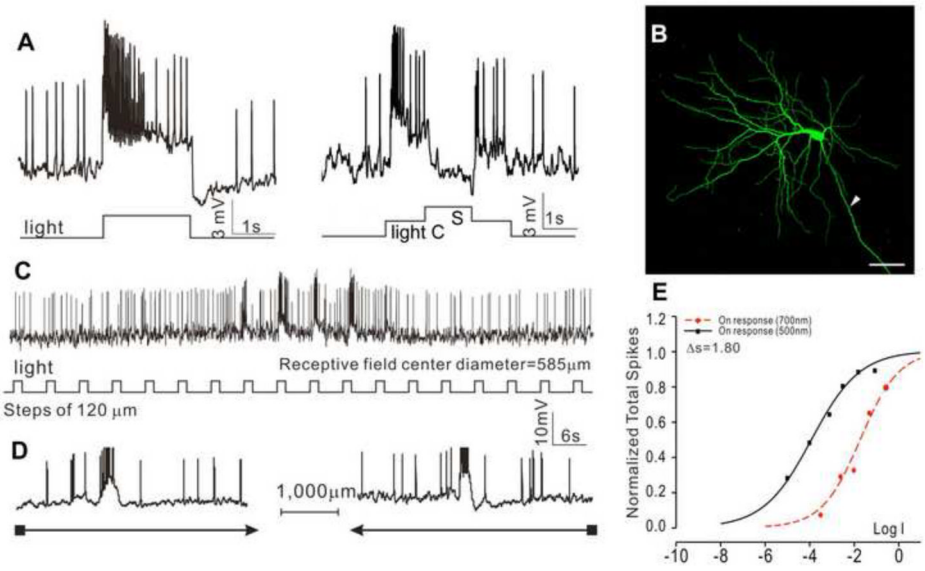

Figure 5.

Voltage responses of a sustained ON-center/OFF-surround GC (sON-c-GC) elicited by whole-field light (-3, 500 nm) (A), and by a center light spot (300 μm) and a surround light annulus (700 μm inner diameter, 2,000 μm outer diameter) (B). (C) Fluorescent micrographs of the GC soma and dendrites (confocal images of the GCL and IPL) stained with neurobiotin (green) by 10-minute dye injection. Dendritic field diameter is 563 μm. Arrowhead: axon. Calibration bar: 100μm, arrowhead: axon. (D) Voltage responses of the AC to a light bar moving stepwise (with 120 μm step increments) across the receptive field. The receptive field center diameter (RFCD) is 585 μm. (E) Voltage responses to a moving light bar in the x and –x directions. (F) Response-intensity (V-Log I) curves of voltage responses to 500 nm and 700nm lights. ΔS is 1.8.

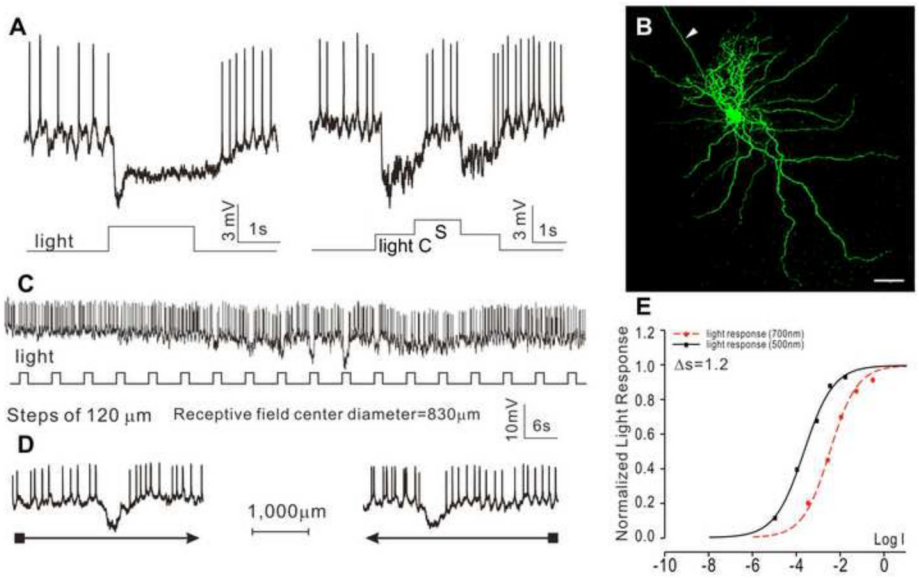

Figure 6.

Voltage responses of a sustained OFF-center/ON-surround GC (sOFF-c-GC) elicited by whole-field light (-3, 500 nm) (A), and by a center light spot (300 μm) and a surround light annulus (700 μm inner diameter, 2,000 μm outer diameter) (B). (C) Fluorescent micrographs of the GC soma and dendrites (confocal images of the GCL and IPL) stained with neurobiotin (green) by 10-minute dye injection. Dendritic field diameter is 800 μm. Arrowhead: axon. Calibration bar: 100μm, arrowhead: axon. (D) Voltage responses of the AC to a light bar moving stepwise (with 120 μm step increments) across the receptive field. The receptive field center diameter (RFCD) is 830 μm. (E) Voltage responses to a moving light bar in the x and –x directions. (F) Response-intensity (V-Log I) curves of voltage responses to 500 nm and 700nm lights. ΔS is 1.2.

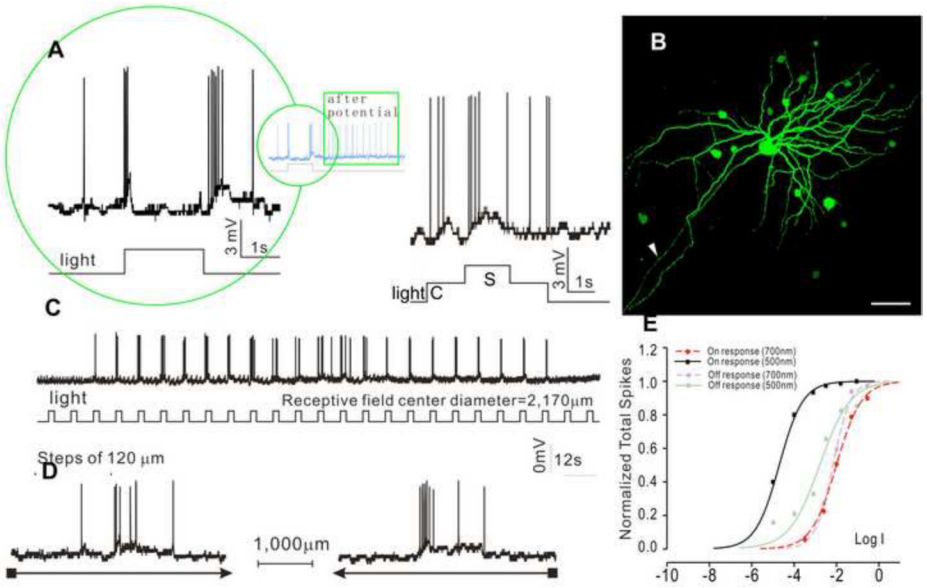

Figure 7.

Voltage responses of transient ON-OFF GC (tON/OFF-GC) elicited by whole-field light (-3, 500 nm) (A), and by a center light spot (300 μm) and a surround light annulus (700 μm inner diameter, 2,000 μm outer diameter) (B). (C) Fluorescent micrographs of the GC soma and dendrites (confocal images of the GCL and IPL) stained with neurobiotin (green) by 10-minute dye injection. Dendritic field diameter is 681 μm. Arrowhead: axon. Calibration bar: 100μm, arrowhead: axon. (D) Voltage responses of the AC to a light bar moving stepwise (with 120 μm step increments) across the receptive field. The receptive field center diameter (RFCD) is 2,170 μm. (E) Voltage responses to a moving light bar in the x and –x directions. (F) Response-intensity (V-Log I) curves of voltage responses to 500 nm and 700nm lights. ΔS is 2.5 for ON response and 0.8 for OFF response.

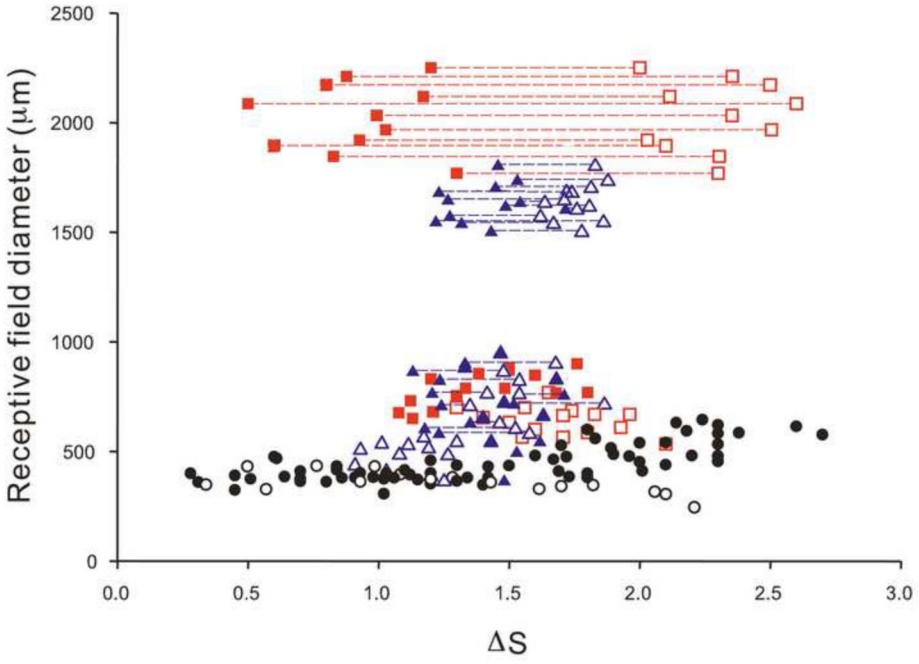

Figure 8.

Scatter plots of receptive field diameter versus spectral difference ΔS of sON-ACs (open blue triangles); sOFF-ACs (solid blue triangles); tON-OFF-ACs (open (ON) and solid (OFF) blue triangles connected by blue dashed lines); tON-OFF-ACws (open (ON) and solid (OFF) blue triangles connected by blue dashed lines); sON-c-GCs (open red squares); sOFF-c-GCs (solid red squares) and tON-OFF-GCs (open (ON) and solid (OFF) red squares connected by red dashed lines). DBCs (open black circles) and HBCs (solid black circles) from a previous publication (Zhang and Wu, 2009a) are also plotted.

Table 1

Number of recorded cells, response waveforms, average spectral difference (ΔS), average dendritic field diameter (DFD), average receptive field diameter (RFD), and presence/absence of center surround antagonism (CSA) and dye coupling of the four types of ACs and three types of GCs.

Cell type	N	Waveform	ΔS	DFD (μm)	RFD (μm)	CSA	Dye coupling
sON-AC	10	Sus. Dep.	1.15±0.69	428±197	435±219	No	No
sOFF-AC	11	Sus. Hyp.	1.49±0.45	408±188	406±247	No	No
tON/OFF-AC	10	Tran.Dep. ON	1.51±0.32	668±226	707±286	No	No
		OFF	1.30±0.27				
tON/OFF-ACw	12	Tran.Dep. ON	1.73±0.51	1,708±278	1,800±186	No	Yes
		OFF	1.54±0.40				
sON-c-GC	15	Dep-c/Hyp-s	1.77±0.68	577±190	585±166	Yes	No
sOFF-c-GC	14	Hyp-c/Dep-s	1.29±0.68	778±144	830±123	Yes	No
tON/OFF-GC	11	Tran.Dep. ON	0.91±0.71	697±254	2,080±311	No	Yes
		OFF	2.20±1.03				

Abbreviations: Sus.Hyp.: sustained hyperpolarization; Tran.Dep.: transient depolarization. N: number of cells, and ±: standard deviation.